LAWRENCE
LIVERMORE
NATIONAL
LABORATORY

UCRL-JRNL-204366

An Evaluation of the Difference Formulation for Photon Transport in a Two Level System

F. D. Daffin, M. S. McKinley, E. D. Brooks, A. Szoke

May 26, 2004

Journal of Computational Physics

An Evaluation of the Difference Formulation for Photon Transport in a Two Level System

Frank Daffin, Michael Scott McKinley, Eugene D. Brooks III and Abraham Szöke

University of California
Lawrence Livermore National Laboratory
Livermore, California 94550

E-mail: daffin1@llnl.gov; mckinley9@llnl.gov; brooks3@llnl.gov; szoke1@llnl.gov

In this paper we extend the difference formulation for radiation transport to the case of a single atomic line. We examine the accuracy, performance and stability of the difference formulation within the framework of the Symbolic Implicit Monte Carlo method. The difference formulation, introduced for thermal radiation by some of the authors, has the unique property that the transport equation is written in terms that become small for thick systems. We find that the difference formulation has a significant advantage over the standard formulation for a thick system. The correct treatment of the line profile, however, requires that the difference formulation in the core of the line be mixed with the standard formulation in the wings and this may limit the advantage of the method. We bypass this problem by using the gray approximation. We develop three Monte Carlo solution methods based on different degrees of implicitness for the treatment of the source terms, and we find only conditional stability unless the source terms are treated fully implicitly.

Key Words: difference formulation; implicit Monte Carlo; line transport

1. INTRODUCTION

Time-dependent transport of radiation from resonance lines is an important component of the physics of stellar atmospheres and of laser-produced plasmas. In optically thick systems, the radiation transport equation for photons is dominated by many spontaneous emission and absorption events and is tightly coupled to the level population equation. This system of equations can be difficult to solve numerically in any discretized scheme in time and space due to its stiffness and the wide range of opacities inherent in an atomic line profile.

It has been known for many years that the explicit Monte Carlo solution of the radiation transport equation, coupled to the material response equation, for a strongly absorbing and emitting material, is numerically unstable. One reason for this is that in optically thick regions both the emission and absorption terms are large and the *net* emission (or absorption) of radiation is a small difference of these two quantities. Any small imbalance

or inconsistency in space and time between absorption and emission terms can lead to instability. This difficulty requires that the source terms in the transport equation be implicitly differenced when using Monte Carlo methods for its solution [1].

The first successful – and now widely used – method for addressing this difficulty came from Fleck and Cummings [2], [3]. Their method, called Implicit Monte Carlo (IMC), converts part of the absorption-emission cycle into instantaneous effective scattering. The net effect of IMC is to reduce the strength of the coupling between the photon transport equation and the material energy equation by peeling off part of the coupling and treating it as effective scattering. Stability is achieved by weakening the radiation-matter coupling. This can lead to unphysical results [4] in addition to a significantly increased execution time to handle the scattered photons.

A second approach to the problem of numerical stability was published in [5] and [6]. In this scheme Monte Carlo particles are emitted and tracked with weights that remain unknown to within a multiplicative factor until the end of the integration cycle. This method, called Symbolic Implicit Monte Carlo (SIMC), removes the costly effective scattering of IMC and does not artificially weaken the radiation-matter coupling. However, in thick systems the strong emission and absorption terms lead to increased Monte Carlo noise.

The difference formulation for photon transport [7] directly addresses the stiffness problem by employing a transformation that replaces the spontaneous emission term with source terms that are small when the local coupling between spontaneous emission and absorption is strong. Our goal, in this paper, is to explore whether or not the difference formulation is cleanly applicable to the case of line transport. We implement and study a numerical application of the difference formulation for the case of the transport of a single atomic line, examining the issues of accuracy, stability and efficiency.

In Section 2 we introduce the equations for line transport first in the standard formulation, and then in the difference formulation. There, a difficulty for the wings of the line appears that would force us to mix the standard formulation with the difference formulation in order to treat a real line profile. We conduct our numerical investigation with a gray (square) line shape function in order to sidestep the issue. The section concludes with a discussion of our treatment of boundary conditions within the new formulation.

Section 3 addresses some details of the numerical treatment of the difference formulation, including the new source terms. The Symbolic Implicit Monte Carlo (SIMC) solution method [5], applied to the standard formulation, requires the solution of a linear system in order to update the atomic populations at the end of the integration cycle. The corresponding population update for the difference formulation is non-linear, requiring a Newton-Raphson solver. Whether or not implicit treatment of the source terms is required in the difference formulation is an open question that we investigate. To this end, we develop three treatments of the source terms, each with differing levels of implicitness. Our explicit treatment is free of a non-linear matrix solve, but is only conditionally stable. Our fully implicit treatment requires a non-linear matrix solve, but numerical evidence suggests that it is unconditionally stable. A semi-implicit method is examined and gives some insight into the numerical instabilities arising in the explicit treatment of the source terms.

We compare the accuracy, efficiency and numerical stability of the SIMC method in the standard formulation to our implementations of the difference formulation in Section 4. We demonstrate that the difference formulation delivers a startling decrease in noise, or an equivalent increase in execution speed for a given noise figure, when compared to

the Monte Carlo solution of the standard formulation for transport. Finally, we present a summary of this work in Section 5.

2. THE EQUATIONS FOR LINE TRANSPORT

We present the transport equations for photons for a two-level atomic system in slab geometry, where the photons are emitted and absorbed according to the same line profile, $\phi(\nu)$, in the regime of complete redistribution. The transport equation for photons is coupled to the population equations for the atomic levels. Motion of the medium and physical scattering of photons are not considered, but we include collisional pumping between atomic levels.

2.1. The standard formulation

In what we refer to as the "standard formulation," we write the photon transport equation as

$$\frac{\partial f}{\partial t} + c\mu\frac{\partial f}{\partial x} = \frac{n_2}{2}A_{21}\phi - c\left(K_{12}n_1 - K_{21}n_2\right)\phi f \quad , \tag{1}$$

where c is the speed of light, x is the position coordinate perpendicular to the slab, μ is the direction cosine of the radiation with respect to x axis, $f(\mu,\nu,x,t)$ is the photon number density distribution per unit atom density, $n_2(x,t)$ is the upper level population fraction, $n_1(x,t)$ is the lower level population fraction, A_{21} is the spontaneous emission rate, $\phi(\nu)$ is the line profile normalized to unit integral [8], and $K_{12} = \kappa N$ where κ is the lower state absorption cross section and N is the atom number density. The coefficient K_{21} satisfies the Einstein relation

$$K_{21} = \frac{g_1}{g_2}K_{12} \quad , \tag{2}$$

where g_1 and g_2 are the statistical weights for levels 1 and 2, respectively. For the purposes of this paper, we consider all material parameters, C_{12}, C_{21}, A_{21}, K_{21} and K_{21} to be independent of x, constant in time, and assume complete redistribution within the line shape.

The equations governing the atomic population fractions n_1 and n_2 are

$$\frac{\partial n_2}{\partial t} = C_{12}n_1 - C_{21}n_2 - A_{21}n_2 + c\left(K_{12}n_1 - K_{21}n_2\right)\int_{-1}^{1}d\mu\int_0^\infty d\nu\,\phi(\nu)f(\mu,\nu) \tag{3}$$

and

$$n_1 + n_2 = 1 \quad , \tag{4}$$

where C_{12} and C_{21} are rate constants for the collisional transitions $1 \rightarrow 2$ and $2 \rightarrow 1$, respectively.

Using Eq. (4), equations (1) and (3) are rewritten as

$$\frac{\partial f}{\partial t} + c\mu\frac{\partial f}{\partial x} = \frac{n}{2}A_{21}\phi - c\left[K_{12} - \left(K_{21}+K_{12}\right)n\right]\phi f \quad , \tag{5}$$

and

$$\frac{\partial n}{\partial t} = C_{12} - \left(C_{12}+C_{21}+A_{21}\right)n + c\left[K_{12} - \left(K_{21}+K_{12}\right)n\right]\int_{-1}^{1}d\mu\int_0^\infty d\nu\,\phi(\nu)f(\mu,\nu) \quad , \tag{6}$$

respectively, where n is the upper level population fraction. We refer to these equations as the standard formulation for line transport in the context of this paper.

2.2. The difference formulation

The difference formulation, introduced in [7], removes the spontaneous emission term and the trouble it causes for thick systems through a simple transformation of the transport equation. The transformation produces a transport equation with new source terms that are small for thick systems, at least in the core of the line, and leads to an efficient numerical solution in optically thick media.

For the case of line transport, the difference formulation is derived by considering the radiation field that is in equilibrium with a given upper level atomic population fraction

$$B(n(x,t)) = \frac{n(x,t)A_{21}}{2c[K_{12} - n(x,t)(K_{21} + K_{12})]} \quad . \tag{7}$$

The equilibrium field, B, defined in Eq. (7) is independent of photon frequency.

We begin the transformation to the difference formulation by rewriting the spontaneous emission term from Eq. (5), as well as from Eq. (6), using the equilibrium field, Eq. (7).

$$\frac{\partial f(x,t;\nu,\mu)}{\partial t} + c\mu\frac{\partial f(x,t;\nu,\mu)}{\partial x} = \\ - c\left[K_{12} - (K_{21} + K_{12})\, n(x,t)\right]\phi(\nu)\left[f\left(x,t;\nu,\mu\right) - B(n(x,t))\right] \quad , \tag{8}$$

$$\frac{\partial n(x,t)}{\partial t} = C_{12} - (C_{12} + C_{21})\, n(x,t) + c\left[K_{12} - (K_{21} + K_{12})\, n(x,t)\right] \\ \times \int_{-1}^{1} d\mu \int_{0}^{\infty} d\nu\, \phi(\nu)\left[f(x,t;\nu,\mu) - B(n(x,t))\right] \; . \tag{9}$$

Next, we define the "difference" intensity,

$$d(x,t;\nu,\mu) = f(x,t;\nu,\mu) - B(n(x,t)) \quad . \tag{10}$$

We note that this is our first sign of trouble for the difference formulation when applied to the case of line transport. The fact that B does not depend upon ν means that in the wings of the line where f is small – even for a system that is thick in the core of the line – the difference field d must be large in order to compensate. The result will be an increase in noise in the wings of the line. We will return to this issue in what follows.

Substituting Eq. (10) into the transport equation gives

$$\frac{\partial f(x,t;\nu,\mu)}{\partial t} + c\mu\frac{\partial f(x,t;\nu,\mu)}{\partial x} = \\ - c\left[K_{12} - (K_{21} + K_{12})\, n(x,t)\right]\phi(\nu) d(x,t;\nu,\mu) \quad . \tag{11}$$

We now subtract the derivatives of B from both sides, giving

$$\frac{\partial d(x,t;\nu,\mu)}{\partial t} + c\mu\frac{\partial d(x,t;\nu,\mu)}{\partial x} = - c\left[K_{12} - (K_{21} + K_{12})\, n(x,t)\right]\phi(\nu) d(x,t;\nu,\mu) \\ - \frac{\partial B(n(x,t))}{\partial t} - c\mu\frac{\partial B(n(x,t))}{\partial x} \quad . \tag{12}$$

The population equation becomes

$$\frac{\partial n(x,t)}{\partial t} = C_{12} - (C_{12} + C_{21})\, n(x,t) + c\,[K_{12} - (K_{21} + K_{12})\, n(x,t)] \int_{-1}^{1} d\mu \int_{0}^{\infty} d\nu\, \phi(\nu) d(x,t;\nu,\mu) \quad . \quad (13)$$

We refer to these equations as the difference formulation of line transport.

Our formal manipulations give us two equivalent forms for the transport and atomic population equations: Eqs. (5), (6) and Eqs. (12), (13). The two sets of equations satisfy equivalent boundary and initial conditions and were obtained without approximation.

2.3. Boundary conditions for the difference formulation

In order to relate the boundary conditions for the standard formulation to those for the difference formulation, we use the fact that the upper level atomic population fraction n is the same for both and use the relation $d = f - B(n)$ to construct the d field from f. The strict non-negativity of f translates into a lower bound for the difference field, $d \geq -B$. When an initial condition is specified for f, the corresponding condition for d can be obtained by the above relation.

In this work the physical medium has finite extent with vacuum boundary conditions. We specify that n be zero in the vacuum and thus $d = f$ there, accordingly. The emission from the surface into the vacuum is given by the $-c\mu\, \partial B/\partial x$ term at the boundaries, in addition to the particles that escape from within. It consists of emission of positive $d = f$ particles into the vacuum, and negative d particles into the material, cooling it, and gives a natural prescription for treating boundary conditions in the difference formulation.

2.4. The gray approximation

The line emission profile $\phi(\nu)$ occurs in both the spontaneous emission and the absorption terms for line transport. This leads to the frequency independence of the equilibrium field, $B(n(x,t))$, and the result that the difference field does not become small in the wings of the line as the optical thickness of the problem is increased. In practical terms, this means that even the simplest line transport problem must employ a mixing of the difference formulation in the core of the line with the standard formulation in the wings.

Wanting to evaluate the effectiveness of the difference formulation in the core of the line, we apply the gray approximation to Eqs. (5) and (6) giving

$$\frac{\partial f}{\partial t} + c\mu \frac{\partial f}{\partial x} = \frac{n}{2} A_{21} - c\,[K_{12} - (K_{21} + K_{12})\, n]\, f \quad , \quad (14)$$

and

$$\frac{\partial n}{\partial t} = C_{12} - (C_{12} + C_{21} + A_{21})\, n + c\,[K_{12} - (K_{21} + K_{12})\, n] \int_{-1}^{1} d\mu\, f(\mu) \quad , \quad (15)$$

respectively. The gray approximation is $\phi(\nu) = 1/w$ for $|\nu - \nu_0| \leq w/2$ and $\phi(\nu) = 0$ for $|\nu - \nu_0| > w/2$, where ν_0 is the line center frequency and w is the line width. Both f and d depend only upon the angle and position, not on frequency, within the line. The line width, w, is factored out of the equations by suitably redefining the fields.

Making the transformation to the difference field, the counterparts to Eqs. (14) and (15) are

$$\frac{\partial d(x,t;\mu)}{\partial t} + c\mu\frac{\partial d(x,t;\mu)}{\partial x} = -c\left[K_{12}-(K_{21}+K_{12})\,n(x,t)\right]d(x,t;\mu) - \frac{\partial B(n(x,t))}{\partial t} - c\mu\frac{\partial B(n(x,t))}{\partial x} \quad , \quad (16)$$

and

$$\frac{\partial n(x,t)}{\partial t} = C_{12} - (C_{12}+C_{21})\,n(x,t) + c\left[K_{12}-(K_{21}+K_{12})\,n(x,t)\right]\int_{-1}^{1} d\mu\, d(x,t;\mu) \quad , \quad (17)$$

respectively. From these equations we develop three Monte Carlo methods based upon different treatments of the source terms $-\partial B/\partial t$ and $-c\mu\,\partial B/\partial x$.

3. NUMERICAL DEVELOPMENT

Let us divide the slab into N zones. The zones are labeled from left to right 1 through N with the position of the left edge of the i^{th} zone labeled x_i. We specify an extra point, x_{N+1}, to mark the position of the right-hand boundary of the slab. We consider n to be piece-wise constant in space within a zone, but allow it to vary continuously in time. Since $B(n)$ behaves likewise, let us write $B_i(t)$ as the value of B in the i^{th} zone at time t. Further, for the purposes of this discussion, let us define B_0 and B_{N+1} for the two boundary regions, representing the boundary conditions to the left and right of the slab respectively, in accordance with our treatment of boundary conditions in the difference formulation introduced in the previous section. Then we may write

$$B(x,t) = B_0 + \sum_{i=1}^{N+1}\left(B_i(t) - B_{i-1}(t)\right)u(x-x_i) \quad , \quad (18)$$

where $u(x)$ is the unit-step function we define as $u(x) = 1$ for $x > 0$, $u(x) = 0$ for $x \leq 0$.

Generally, the total Monte Carlo weight to be emitted from a source S is given by the integral

$$W = \int_R S\, dR \quad , \quad (19)$$

where R is the finite volume element of the relevant phase space used in the numerical model and dR is its infinitesimal. For this model R is $2\Delta x\Delta t$, and so we may write

$$W^t = -\int_{\mu=-1}^{\mu=+1} d\mu \int_{\Delta x} dx \int_{\Delta t} dt\, \frac{\partial B}{\partial t} \quad , \quad (20)$$

and

$$W^x = -c\int_{\mu=-1}^{\mu=+1} d\mu \int_{\Delta x} dx \int_{\Delta t} dt\, \mu\frac{\partial B}{\partial x} \quad , \quad (21)$$

where the superscripts t and x indicate the weight emitted by the $-\partial B/\partial t$ and the $-c\mu\,\partial B/\partial x$ source, respectively. The probability distribution function of the physical

variables to be sampled is given by

$$g = \frac{S}{W} \quad , \tag{22}$$

for a source S emitting weight W. We use these relations to develop the foundation for three Monte Carlo methods for solving the difference formulation for atomic line transport, Eqs. (16) and (17).

3.1. Source Terms

The spontaneous emission term, $nA_{21}/2$, in the standard formulation, Eq. (14), is replaced by two new source terms, namely $-\partial B/\partial t$ and $-c\mu\,\partial B/\partial x$, in the difference formulation, Eq. (16). The new source terms play different roles than the spontaneous emission term of the standard formulation. The $-c\mu\,\partial B/\partial x$ term is responsible for driving the transport of the d field through the slab, and the $-\partial B/\partial t$ term acts to compensate for changes in the reference field $B(n)$ by changing the d field in order to hold f fixed.

3.1.1. Source term $-\partial B/\partial t$

We evaluate Eq. (20) for a given zone i giving the weight to be accorded to the $-\partial B/\partial t$ source term:

$$W_i^t = -\int_{\mu=-1}^{\mu=+1} d\mu \int_{\Delta x_i} dx \int_{t_0}^{t_0+\Delta t} dt \left(\frac{\partial B}{\partial t}\right)_i = -2\Delta x_i \left[B_i(t_0+\Delta t) - B_i(t_0)\right] \quad , \tag{23}$$

where we have used the piece-wise constant property of B in the integral over Δx_i.

Now we may write the distribution function for the source in zone i using Eq. (22)

$$g_i^t = \frac{\left(\partial B/\partial t\right)_i}{2\Delta x_i \left[B_i(t_0+\Delta t) - B_i(t_0)\right]} \quad . \tag{24}$$

Further development of the distribution function depends upon assumptions about the nature of the differencing employed and varies with our construction of the Monte Carlo methods we use for the difference formulation. We will address the details of our construction later in this work.

3.1.2. Source term $-c\mu\,\partial B/\partial x$

Now let us consider the space-derivative term. Due to the piece-wise constant treatment of n, this source term is non-zero only at a discontinuity in the value of n between two adjoining zones or at a discontinuity between the surfaces of the slab and its surroundings.

The derivative $\partial B/\partial x$ gives

$$\frac{\partial B}{\partial x} = \sum_{i=1}^{N+1} \left(B_i(t) - B_{i-1}(t)\right) \delta(x - x_i) \quad , \tag{25}$$

where δ is the Dirac delta function.

Since $-c\mu\,\partial B/\partial x$ is an odd function of μ in slab geometry, the sum of the weight emitted from this source over all angles $\{\theta : \mu = \cos\theta\}$ is zero. Nevertheless, it is not correct to ignore the source; $-c\mu\,\partial B/\partial x$ is responsible for driving the transport of d particles through the slab. Our solution is to emit d-particle pairs of equal and opposite weight in

$+\mu$ and $-\mu$ directions, thereby assuring that zero net weight is emitted without statistical noise.

To find the weight to be emitted, say in the $+x$ direction in the i^{th} zone, we integrate the $-c\mu\,\partial B/\partial x$ source from $\mu = 0$ to $\mu = 1$

$$W_i^{+x} = -c \int_{\mu=0}^{\mu=1} \mu\, d\mu \int_{t_0}^{t_0+\Delta t} dt \int_{x_i}^{x_i+\Delta x_i} dx\, \delta(x - x_i)[B_i(t) - B_{i-1}(t)] = \\ - \frac{c}{2} \int_{t_0}^{t_0+\Delta t} dt\, [B_i(t) - B_{i-1}(t)] \quad . \quad (26)$$

Weight emitted in the $-x$ direction is identical, except for a change in sign.

Now we may write the distribution function for the source in the $+x$ direction in zone i using Eq. (22)

$$g_i^{+x} = \frac{2\mu\delta(x - x_i)\,[B_i(t) - B_{i-1}(t)]}{\int_{t_0}^{t_0+\Delta t} dt\ [B_i(t) - B_{i-1}(t)]} \quad . \quad (27)$$

The presence of the δ-function tells us that the particles are to be emitted at zone boundaries. Emission angles are sampled according to $\mu = \sqrt{\rho}$, where ρ is a random variate uniformly distributed between 0 and 1.

3.2. Solution methods

We construct three different Monte Carlo solution methods employing the difference formulation for the transport of an atomic line. In the construction we address the details of the treatment of the source terms. The solution methods utilize different degrees of implicit treatment of the source terms, with each succeeding method being more implicit than the one before it.

We begin by integrating Eq. (17) over a time step, approximating $n(t)$ by $n(t_0 + \Delta t)$ in the collision (pumping) terms and by $n(t_0)$ in the absorption term, giving

$$n(x, t_0 + \Delta t) = n(x, t_0) + [C_{12} - (C_{12} + C_{21})\, n(x, t_0 + \Delta t)]\, \Delta t \\ + c\,[K_{12} - (K_{21} + K_{12})\, n(x, t_0)] \int_{t_0}^{t_0+\Delta t} dt \int_{-1}^{1} d\mu\, d\,(x, t; \mu) \quad , \quad (28)$$

where t_0 is the census time of the previous Monte Carlo integration cycle and $t_0 + \Delta t$ is the census time of the current cycle. This intermediate step is the common point of departure for the three Monte Carlo solution methods.

We would like to note that for the difference formulation the source terms of the transport equation, Eq. (16), do not appear in the material response equation, Eq. (17), and are likewise absent in Eq. (28). This is in contrast to Eqs. (14) and (15), where the spontaneous emission term, $A_{21}n$, appears in both the transport and the material response equation, causing stiff coupling between them. The self-consistent differencing of the spontaneous emission term in Eqs. (5) and (6), for the purpose of stability, leads to effective scattering in the IMC method discussed in [3], and the linear system solve in the SIMC method discussed in [5].

3.2.1. The explicit solution method

In this method there is no implicit treatment of the sources and, unlike SIMC, it does not require the inversion of a matrix at the end of each Monte Carlo integration cycle in order

to calculate $n_i(t_0 + \Delta t)$. In this scheme $-c\mu\,\partial B/\partial x$ is explicitly differenced at time t_0, and the action of $-\partial B/\partial t$ is delayed until the end of the integration loop, at which point $n(t_0 + \Delta t)$ is available.

Starting with the $-\partial B/\partial t$ source for zone i, we approximate

$$\left(\frac{\partial B}{\partial t}\right)_i \approx \frac{B_i(t_0 + \Delta t) - B_i(t_0)}{\Delta t} \quad . \tag{29}$$

Substituting this result into Eq. (24) gives

$$g_i^t = \frac{1}{2\,\Delta x_i\,\Delta t} \quad , \tag{30}$$

which directs us to distribute the weight given in Eq. (23) evenly within the zone.

Considering the $-c\mu\,\partial B/\partial x$ source, we take $B_i(t) \rightarrow B_i(t_0)$, the value of B_i at the beginning of the time interval. Substituting this into Eq. (26) gives

$$W_i^{+x} = -\frac{c\,\Delta t}{2}\left[B_i(t_0) - B_{i-1}(t_0)\right] \quad , \tag{31}$$

for emission in the $+x$-direction. And Eq. (27) becomes

$$g_i^{+x} = \frac{2\mu\delta(x - x_i)}{\Delta t} \quad , \tag{32}$$

where the weight of the source is to be distributed evenly throughout the time interval Δt, but the emission is to take place on the zone boundary x_i.

At the beginning of each iteration of the Monte Carlo integration loop, difference particles from the $-c\mu\,\partial B/\partial x$ source are emitted at the zone boundaries using $B(t_0)$, and distributed uniformly in time across the time step interval Δt. The particles are then propagated to census time, $t_0 + \Delta t$, according to Eq. (16) before $n(t_0 + \Delta t)$ is calculated.

To obtain $n_i(t_0 + \Delta t)$, write Eq. (28) as

$$n_i(t_0 + \Delta t) = \gamma n_i(t_0) + \gamma C_{12}\Delta t + \frac{\gamma c}{\Delta x_i}[K_{12} - (K_{21} + K_{12})n_i(t_0)]\mathsf{D}_i \quad , \tag{33}$$

where i is the zone index, Δx_i is the width of the zone,

$$\gamma = \frac{1}{[1 + (C_{12} + C_{21})\Delta t]} \quad , \tag{34}$$

and where

$$\mathsf{D}_i = \int_{\Delta t} dt \int_{\Delta x_i} dx \int_{-1}^{1} d\mu\, d\,(x, t; \mu) \tag{35}$$

is the time integral of the d-field calculated from Monte Carlo particles traveling through zone i during the time step.

Now that we have an estimate of $n_i(t_0 + \Delta t)$ from Eq. (33), difference particles sample the $-\partial B/\partial t$ source with the total weight given by Eq. (23) and are evenly distributed in space within a zone. This emission is not evenly distributed across the time step, it has a time coordinate of $t_0 + \Delta t$, the census time of the current integration interval. This sequence is then repeated for the next time step.

3.2.2. The semi-implicit solution method

We call this method "semi-implicit" because we implicitly difference the $-\partial B/\partial t$ source term, but explicitly difference the $-c\mu\,\partial B/\partial x$ source term. The implicit differencing of the $-\partial B/\partial t$ source term leads to a matrix solve at the end of each iteration of the Monte Carlo integration loop. Our purpose in examining this method is to provide insight into the sources of numerical instability of the fully explicit method described above. Once one must pay the cost of the non-linear matrix solve, one might as well extract the benefits of a fully implicit solution method.

In this semi-implicit treatment of the source terms for the difference formulation, the emission from $-\partial B/\partial t$ is calculated at the start of the integration loop, not postponed until the end as in the explicit scheme just discussed. The weight emitted is given by Eq. (23). However, $B_i(t_0+\Delta t)$ is unknown at this point, and a portion of the weight, $-2\Delta x_i$, is "symbolic" in the same vein as in [5] and requires a non-linear matrix solve at the end of each Monte Carlo integration cycle. The remaining portion, $2\Delta x\, B_i(t_0)$, contains no unknown factors and provides known (numeric) contributions to the d-field. The particles are created with time coordinates uniformly distributed over the interval Δt as dictated by Eq. (30), in contrast to the explicit case where their time coordinates are set to census time.

Next, the $-c\mu\,\partial B/\partial x$ source is sampled in the same way as in the explicit treatment above, and d-particles with weight given by Eq. (31) are created. These particles, fully numeric contributions to the d-field, are distributed in space, time and direction according to Eq. (32).

This treatment of the source terms leads to the following representation of Eq. (28):

$$n_i(t_0+\Delta t) = \gamma n_i(t_0) + \gamma C_{12}\Delta t + \frac{\gamma c}{\Delta x_i}\left[K_{12} - (K_{21}+K_{12})n_i(t_0)\right] \times \left[\mathsf{D}_i + \sum_{j=1}^{N} \mathcal{D}_{ij}\, B_j(t_0+\Delta t)\right] \quad . \tag{36}$$

Here $\mathcal{D}_{ij}$ is the symbolic contribution to the $i^{\rm th}$ zone from particles born in the $j^{\rm th}$ zone, and D_i is the contribution to zone i coming from particles with numeric weights in much the same way as in Eq. (33), including the numeric contributions from $-\partial B/\partial t$ and $-c\mu\,\partial B/\partial x$ sources. The sole contributor to symbolic energy depositions is the forward-differenced portion of $-\partial B/\partial t$.

Since B is non-linear in n, then Eq. (36) represents a non-linear system that must be solved for $n_j(t_0+\Delta t)$ at the end of each cycle through the integration loop, whereas the equivalent expression in [5] represented a system linear in n. We iterate the Newton-Raphson algorithm to solve the non-linear system for $n_j(t_0+\Delta t)$, and then use $B(n_j(t_0+\Delta t))$ to convert the Monte Carlo particles with symbolic weights to numeric weights. In this way the d-field, at census, is fully numeric and free of unknown factors before the next iteration of the Monte Carlo integration loop.

3.2.3. The implicit solution method

We call this method "implicit" because we treat the $-c\mu\,\partial B/\partial x$ implicitly in time. By taking $B_i(t) \rightarrow B_i(t_0+\Delta t)$, instead of $B_i(t) \rightarrow B_i(t_0)$ as in the last two methods introduced above, Eq. (26) becomes

$$W_i^{+x} = -\frac{c\,\Delta t}{2}\left[B_i(t_0+\Delta t) - B_{i-1}(t_0+\Delta t)\right] \quad . \tag{37}$$

Eq. (32) remains unchanged.

The sequence of calculations in the integration loop is similar to that used in the semi-implicit method above. First, particles sampling the $-\partial B/\partial t$ source are emitted with a portion of their weight numeric, $-2\Delta x_i\, B_i(t_0)$, and the remainder symbolic, $-2\Delta x_i$, according to Eq. (23) and exactly like the semi-implicit method. Next, $-c\mu\,\partial B/\partial x$ is sampled according to Eq. (32), but in this case the weight is purely symbolic.

We write Eq. (28) as

$$n_i(t_0+\Delta t) = \gamma n_i(t_0) + \gamma C_{12}\Delta t + \frac{\gamma c}{\Delta x_i}\left[K_{12} - (K_{21}+K_{12})n_i(t_0)\right] \times \left\{ \mathsf{D}_i + \sum_{j=1}^{N} \mathcal{D}^t_{ij}\, B_j(t_0+\Delta t) + \sum_{k=1}^{N+1} \mathcal{D}^x_{ik}\left[B_k(t_0+\Delta t) - B_{k-1}(t_0+\Delta t)\right] \right\} \quad (38)$$

where we introduce the new symbolic contribution, $\mathcal{D}^x_{ik}$, of the $-c\mu\,\partial B/\partial x$ source emitted from zone k and propagated to zone i, where $[B_k(t_0+\Delta t) - B_{k-1}(t_0+\Delta t)]$ is the factor necessary to convert that symbolic weight into numeric weight. One may consider the last summation as one over zone interfaces while remembering that the index k in B_k and B_{k-1} refers to zone indices. The term $\mathcal{D}^t_{ij}$ represents the symbolic contribution of the $-\partial B/\partial t$ source, the D_i term includes the numeric contributions from $-\partial B/\partial t$ sources, and $B_j(t_0+\Delta t)$ plays the same role in this equation as it does in Eq. (36). B_0 and B_{N+1} are prescribed boundary conditions.

4. NUMERICAL RESULTS IN THE GRAY APPROXIMATION

We select the SIMC solution method in the standard formulation as a point of comparison for the difference formulation [7]. We discuss the numerical accuracy and efficiency, and report on the numerical stability of each of the three Monte Carlo solution methods we developed in the previous section, with emphasis on exploring the stability characteristics of the fully explicit version, itself free of a matrix solve at the end of each integration cycle, relative to the SIMC treatment of the standard formulation for a range of optical thicknesses. We do not address the issue of teleportation error [9] in this work. For the sake of brevity, we refer to each of the Monte Carlo solution methods we developed above for the difference formulation for atomic line transport as one of a trio of "difference methods" and to SIMC for the standard formulation as the "standard method." The problems were run until equilibrium was reached.

4.1. Relative accuracy and efficiency

Table I lists the parameters describing the initial and boundary conditions and the material parameters we use in comparing the SIMC method (standard method) for the standard formulation to each of the three Monte Carlo methods (difference methods) developed in the previous section for the difference formulation. In all calculations the slab is initialized with $n = 0.25$ for all zones and the photon fields $f(t=0) = 0$. This initial state for the photon field, f, corresponds to a non-zero initial difference field, d, which must be sampled to properly initialize the system. While this provides a net zero photon field in each zone, the statistical nature of sampling leads to small, local fluctuations. As we will show, this in turn can lead to differences among the methods in their transient behavior, even in the limit of short time steps.

The optical depth for this model depends on the value of $n(x,t)$. We first tune the input parameters using the standard method to obtain the desired nominal optical depth, then use the same input values for the difference methods.

TABLE I
Input parameters used for all Monte Carlo solution methods describing the initial conditions, boundary conditions, and material properties of the unit slab.

Parameter	Value			
	Nominal Optical Depth $= 1$	Nominal Optical Depth $= 10$	Nominal Optical Depth $= 100$	Nominal Optical Depth $= 1000$
$n(0 \leq x \leq 1, t = 0)$	.25	.25	.25	.25
$f(x, \mu, t = 0)$	0	0	0	0
$n(x < 0, t)$	0	0	0	0
$n(x > 1, t)$	0	0	0	0
K_{12}	1.125	18	207.5	2155
K_{21}	1.125	15.3422	207.5	2155
C_{12}	0.245423	0.245423	0.245423	0.245423
C_{21}	0.667128	0.667128	0.667128	0.667128

In order to more faithfully reproduce the boundary layer near the edges of the slab for thicker problems, we find it necessary to modify the zoning, depending upon optical thickness, and this can influence execution time. Since the gradient of n in space varies slowly and more uniformly over the length of the slab in the thin problems – optical thicknesses 1 and 10 – we model the slab using 21 zones of uniform size in thin systems. However, for thick problems – optical thicknesses of 100 and 1000 – gradients in n are concentrated in the boundary layers. For these we use small zones in the boundary layers and increase their size in a geometric progression towards the center of the slab. Thus, we can compare accuracy and efficiency among methods for a given optical thickness only.

4.1.1. Relative accuracy

Table II demonstrates the accuracy of the three Monte Carlo solution methods relative to the SIMC method for a simple, two-level, system in slab geometry. The data consist of the means and standard deviations of 120 statistically independent calculations of the optical thickness of the slab for each method, in equilibrium, for the fixed input parameters shown in Table I. The results show that the means of the calculated optical thicknesses are within one standard deviation of each other. Therefore, the results are statistically consistent with the assertion that all three Monte Carlo solution methods in the difference formulation converge to the same result as SIMC in the standard formulation in equilibrium. It is interesting to note that the standard deviations of the difference methods are approximately independent of optical depth, whereas those of SIMC increase several orders of magnitude as optical depth increases.

4.1.2. Relative efficiency

The variance in a Monte Carlo calculation scales inversely with the number of particles used, in the limit of large particle count. We use this fact as a means to evaluate the relative efficiency of the methods for a given discretization of the problem. We match the run-times among the methods by adjusting the number of Monte Carlo particles used in each, taking care to ensure that the Monte Carlo effort dominates the calculation and that the variance scales appropriately with the number of Monte Carlo particles. Then the variances of the

TABLE II
The means and standard deviations of the optical thickness of a unit slab calculated using each of the three difference methods and the standard method, at equilibrium. All calculations are matched in execution time.

Nominal Optical Thickness	Difference Method: Explicit	Difference Method: Semi-Implicit	Difference Method: Implicit	Standard Method
1	$1.0087 \pm 2 \times 10^{-4}$	$1.0088 \pm 1 \times 10^{-4}$	$1.0087 \pm 1 \times 10^{-4}$	$1.00873 \pm 8 \times 10^{-5}$
10	$10.067 \pm 1 \times 10^{-3}$	$10.067 \pm 1 \times 10^{-3}$	$10.0671 \pm 9 \times 10^{-4}$	$10.067 \pm 4 \times 10^{-3}$
100	$98.655 \pm 1 \times 10^{-3}$	$98.654 \pm 1 \times 10^{-3}$	$98.653 \pm 1 \times 10^{-3}$	$98.65 \pm 8 \times 10^{-2}$
1000	$998.726 \pm 1 \times 10^{-3}$	$998.726 \pm 1 \times 10^{-3}$	$998.7263 \pm 9 \times 10^{-4}$	$998.7 \pm 9 \times 10^{-1}$

calculations are inversely proportional to the relative efficiencies of the methods. This is how we estimate the run-time advantage of the difference methods over the standard method.

Table III consists of the variances of the optical depths presented in Table II, and Table IV shows the calculated speed-up factors, based upon the measurements in Table III. All three difference methods show a clear run-time advantage over the standard formulation for thick systems. The advantage is striking at an optical depth of 1000 mean free paths. However, as Table IV shows, for thin problems the advantage diminishes and is lost completely somewhere between optical depths of 10 and 1, corresponding to a per-zone optical depth of 0.5 and 0.05, respectively. For thick systems, the desired statistical accuracy is achieved with a much lower particle count.

TABLE III
The variances of the optical thickness of a unit slab calculated using the three difference methods and the standard method, at equilibrium.

Nominal Optical Thickness	Difference Method: Explicit	Difference Method: Semi-Implicit	Difference Method: Implicit	Standard Method
1	3.0×10^{-8}	1.5×10^{-8}	1.4×10^{-8}	6.0×10^{-9}
10	1.1×10^{-6}	1.0×10^{-6}	8.2×10^{-7}	1.8×10^{-5}
100	1.1×10^{-6}	1.2×10^{-6}	9.3×10^{-7}	6.9×10^{-3}
1000	9.6×10^{-7}	1.0×10^{-6}	6.0×10^{-7}	8.7×10^{-1}

TABLE IV
Speed-up factors of the three difference methods over the standard method for various nominal optical thicknesses.

Nominal Optical Thickness	Difference Method: Explicit	Difference Method: Semi-Implicit	Difference Method: Implicit
1	2.0×10^{-1}	4.0×10^{-1}	4.3×10^{-1}
10	1.6×10^{1}	1.8×10^{1}	2.2×10^{1}
100	6.3×10^{3}	5.8×10^{3}	7.4×10^{3}
1000	9.1×10^{5}	8.7×10^{5}	1.5×10^{6}

4.2. Transient behavior of the difference and standard formulations

While we do not expect two different solution methods, such as the standard method and any one of the three difference methods, to behave identically during the first few time steps of the integration, we do expect their behaviors to converge for sufficiently small time step sizes.

This is indeed the case. Figures 1 through 4 show the transient behavior of $n(t)$, the fraction of atoms in the excited state, in the central zone of a slab with an optical thickness of 10 mean free paths at equilibrium. Figures 1 through 3 show the transient behavior of each of the three difference methods, with Figure 4 showing the transient behavior of the standard method. Each figure shows graphs of $n(t)$ calculated with different time step sizes in units of $(slab\ length)/c$, where c is the speed of light in the material (set to 1 in this work).

Initially the slabs have uniform excitation energies corresponding to $n(x, t = 0) = 0.25$, but there are no photon fields. At the start, the radiation field and the material energy are out of equilibrium, with n falling initially in order to bring about radiative equilibrium. The motion of n is then driven by the net collisional excitation and absorption, recovering on a longer time scale. Each of the difference methods and the standard method show this behavior and agree qualitatively. Note the overshoot in the standard formulation and explicit implementation of the difference formulation for long time steps. Their quantitative agreement improves with decreasing time step sizes, and Figure 5 shows good overlap among the four methods for a time step size of 0.00625.

Aside from the noise apparent in the standard method as the magnitude of the photon field grows, there is a small but discernible difference in the minimum of $n(t)$ among the four methods. We believe this is due to sampling noise. Recall that initializing the photon field to zero in the difference formulation requires sampling $d(t = 0)$ so that $f = d + B(t = 0) = 0$. Statistical fluctuations in the Monte Carlo sampling of the physical coordinates of the particles composing this initial d-field leads to small, localized fluctuations that can affect n shortly after $t = 0$.

Table V shows the average and one standard deviation of the minimum n reaches for 200 statistically independent calculations using each of the three difference methods and the standard method, all matched in execution time. The time step size used in each calculation is 0.00625, the same as in Figure 5. Also shown are the average and standard deviation of the times at which n reached its nadir in the calculations. Table V shows that the three difference methods and the standard method produce minima of the same magnitude and at the same time, within the estimated uncertainties. Thus we show that not only do the difference methods agree with the standard method in equilibrium (see Table II) they also agree in the transient behavior of n for sufficiently small time step sizes.

4.3. Numerical stability of the difference formulation

We explore the stability characteristics of the three different treatments of the source terms in the difference formulation for line transport. Of particular interest is the numerical stability of the explicit treatment, since it is free of a matrix solve in the Monte Carlo integration cycle and will thus remain economical as the number of zones in the problem increases. We find the implicit treatment, Eq. (38), for the difference formulation to be numerically stable for optical thicknesses ranging from 1 to 1000, even for time step sizes on the order of 10 light travel times across the slab, and we expect the treatment to remain stable for thicker systems. This provides numerical evidence that this treatment

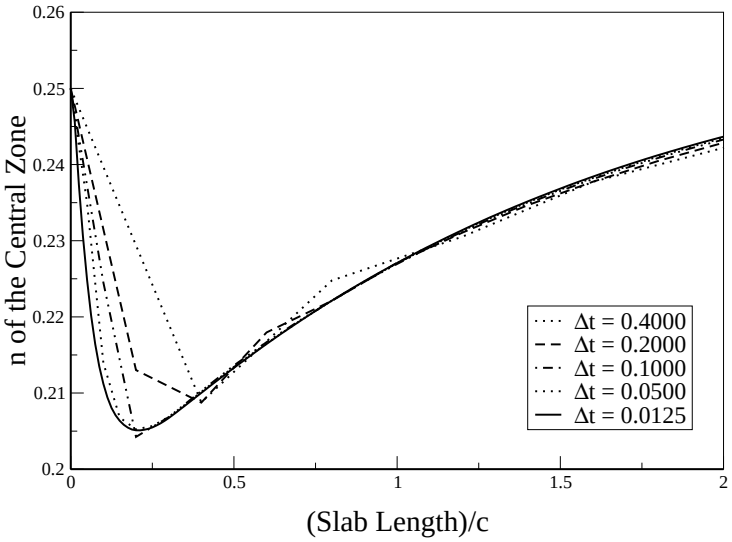

FIG. 1. Transient behavior of $n(t)$ – the fraction of atoms in the excited state – in the central zone for the explicit difference method.

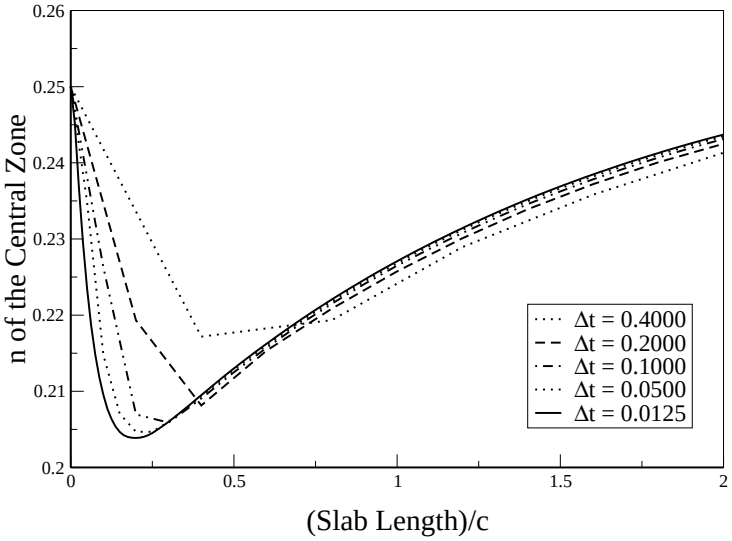

FIG. 2. Transient behavior of $n(t)$ – the fraction of atoms in the excited state – in the central zone for the semi-implicit difference method.

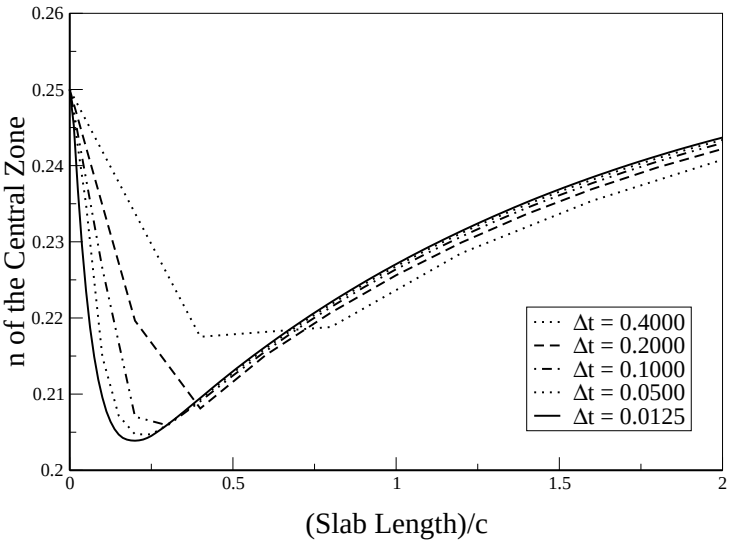

FIG. 3. Transient behavior of $n(t)$ – the fraction of atoms in the excited state – in the central zone for the implicit difference method.

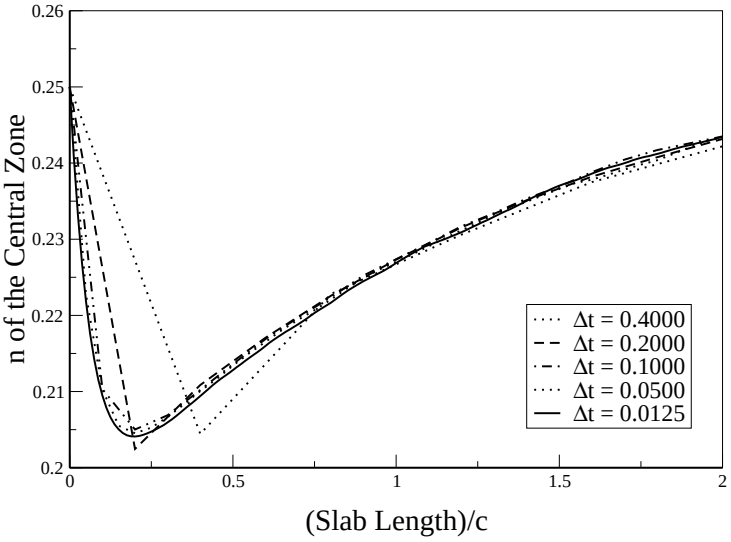

FIG. 4. Transient behavior of $n(t)$ – the fraction of atoms in the excited state – in the central zone for the standard method.

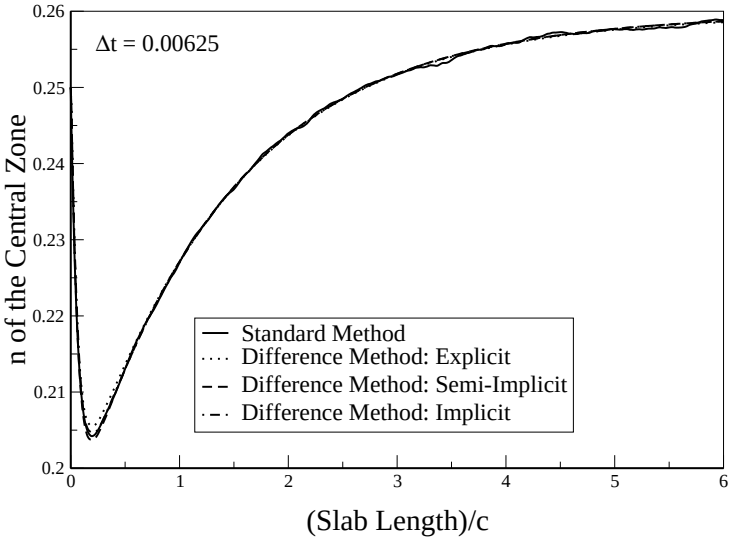

FIG. 5. Transient behavior of n – the fraction of atoms in the excited state – of the three difference methods and the standard method.

TABLE V
The mean and standard deviation of the minimum n and the time of its nadir. Quantities were calculated using the three versions of the difference method and the standard method.

Monte Carlo Solution Methods	Minimum n	Time of nadir of n
Difference Method: Explicit	0.204 ± 0.001	0.197 ± 0.008
Difference Method: Semi-Implicit	0.204 ± 0.001	0.196 ± 0.008
Difference Method: Implicit Scheme	0.204 ± 0.001	0.196 ± 0.008
Standard Method	0.2041 ± 0.0001	0.193 ± 0.004

of the source terms is unconditionally stable. We find that both the explicit and the semi-implicit treatments, Eqs. (33) and (36), respectively, are only conditionally stable. For these treatments of the source terms, stability depends upon the optical depth of the slab, the size of the zones, and the size of the time step. Figures 6 and 7 show the approximate neighborhood of the onset of instability for both treatments. The methods are numerically unstable in the regions above their graphs. Beyond a certain optical thickness, the systems become stable for practically any time step size, so the graphs terminate. The calculations were run until the systems were well equilibrated. Whereas the explicit differencing of the standard formulation is known to be stable for thin and unstable for thick systems [2], we find the contrary for the semi-implicit and fully explicit difference methods. Thus, in the explicit treatment of the difference formulation it appears that we trade numerical stability in thin systems for numerical stability in thick systems.

Figures 6 and 7 show that the regions of stability for both the explicit and the semi-implicit methods are similar in shape. It is apparent in both figures that the explicit

treatment requires shorter time steps in order to obtain stability. For thin systems the stability of both treatments is insensitive to the zone size, as shown in Figure 7. For thick systems the constraint on the time step size in order to obtain stability is relaxed as the zone size is increased. Both figures demonstrate that the optical thickness of the zones is an important factor in the stability of the calculations.

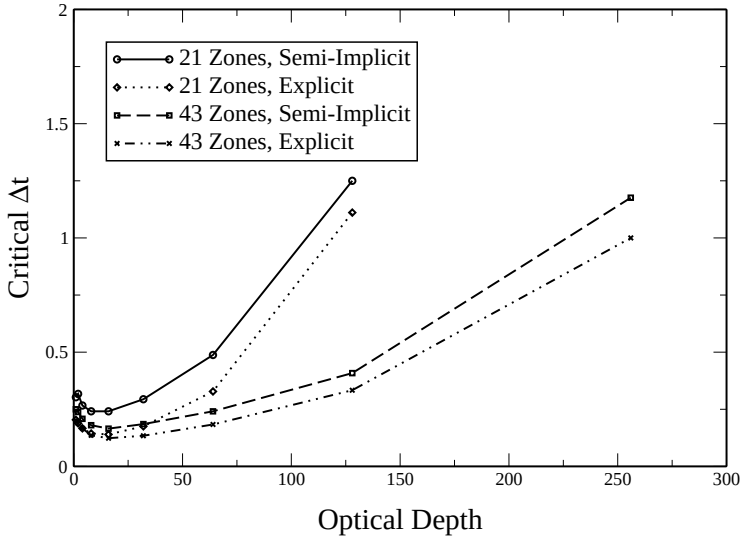

FIG. 6. Graphs of the time step size versus optical depth of the slab near the edge of numerical stability for the explicit and semi-implicit difference methods. Two zone thicknesses are shown. The vertical axis is in units of $(slab\ length)/c$. Instability for a given treatment of the source terms occurs above the line. Beyond the termination of the lines, the calculations are stable for any time step.

It is interesting to note the weakness of the dependence of both the semi-implicit and explicit treatments of the source terms on the zone size, Δx, for thin systems. Terms in the finite difference equations, Eqs. (33) and (36), that depend upon zone size have little apparent influence upon the stability of those solution methods. Additionally, since both treatments of the source terms have similar regions of stability, a formal stability analysis of the simpler explicit formulation may give insight into the stability criterion of the more complicated, semi-implicit method.

For the slab geometry, collisional-pumped, line-trapping problems studied here, the explicit treatment of the source terms, unencumbered by a non-linear system solve at each time step, appears no more economical than the semi-implicit method, which is more stable. One should consider, however, that the cost of the non-linear system solve grows rapidly as one scales the number of zones in the problem. Further, while the implicit scheme demonstrates superior stability characteristics, it too relies upon a non-linear system solve at each time step. Since the primary difference between the conditionally stable methods and the apparently unconditionally stable implicit method is the explicit treatment of the $-c\mu\,\partial B/\partial x$-term, we believe that it is responsible for driving the numerical instability in the explicit and semi-implicit treatments of the source terms.

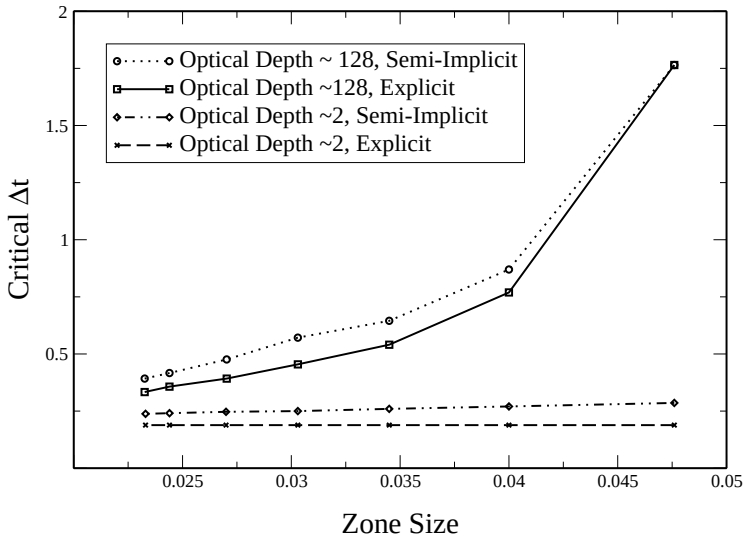

FIG. 7. Graphs of the time step size versus zone size near the edge of stability for the explicit and semi-implicit difference methods. The slabs are divided into zones of uniform size and two optical depths for each scheme are shown. The vertical axis is in units of $(slab\ length)/c$, and the horizontal axis is in fractions of the total length of the unit slab.

5. CONCLUDING REMARKS

In this paper we examined the accuracy and performance of the difference formulation [7] relative to the Symbolic Implicit Monte Carlo (SIMC) [5] solution method applied to the standard formulation of photon transport in a strongly absorbing/emitting two level system using the gray approximation. We developed three different numerical treatments of the difference formulation and presented evidence of their superior computational efficiency for thick systems. We found that to an equivalent noise figure, the difference methods were 10^6 times faster than the standard method for slabs 1000 mean free paths thick, or equivalently, provide a 10^3 reduction in Monte Carlo noise for a given execution time.

We demonstrated that the three implementations of the difference formulation we developed were in excellent agreement with the SIMC implementation of standard formulation. Additionally, we showed through a detailed comparison that while their transient behavior differs for large time steps there is good numerical evidence that all the treatments of the source converge for sufficiently small time steps.

We found that the fully implicit version of the difference formulation is stable, and we believe it to be unconditionally so. The fully explicit version, although free of any matrix solve, is only conditionally stable. Moreover, it possess a stability region similar to the semi-implicit difference method which may provide insight into a formal stability analysis. For both conditionally stable versions of the difference formulation, stability appears to depend strongly upon the optical thickness of the zones dividing the material. Finally, we believe that it is the explicit treatment of the $-c\mu\,\partial B/\partial x$ term that drives the instability in the explicit difference method.

As a final note, the explicit treatment of the source terms in the standard formulation is stable in the limit of optically thin systems, while the explicit source term treatment of the difference formulation is stable in the limit of optically thick systems. This leaves open the possibility that the non-linear matrix solve might be avoided when applying the difference formulation to practical problems involving thick media.

REFERENCES

1. T. N'Kaoua and R. Sentis, A New Time Discretization for the Radiative Transfer equations: Analysis and Comparison with the Classical Discretization, *SIAM Journal on Numerical Analysis*, Vol. 30, 733-748 (1993).
2. J. A. Fleck, Jr and J. D. Cummings, An implicit Monte Carlo scheme for calculating time and frequency dependent non linear radiation transport, *Journal of Computational Physics*, Vol. 8, 1971, pp. 313-342.
3. E. D. Brooks III and J. A. Fleck, Jr., An Implicit Monte Carlo Scheme for Calculating Time-Dependent Line Transport, *Journal of Computational Physics*, Vol. 67, No. 1, November 1986, pp. 59-72.
4. Densmore J.D., Larsen E. W., *Asymptotic Equilibrium Diffusion Analysis of Time-Dependent Monte Carlo Methods for Grey Radiative Transfer*, Journal of Computational Physics (in press), Los Alamos National Laboratory preprint LA-UR-03-9164.
5. E. D. Brooks III, Symbolic Implicit Monte Carlo, *Journal of Computational Physics*, Vol. 83, No. 2, August 1989, pp. 433-446.
6. T. N'Kaoua, Solution of the Nonlinear Radiative Transfer Equations by a Fully Implicit Matrix Monte Carlo Method Coupled with the Rosseland Diffusion Equation Via Domain Decomposition, *SIAM Journal Scientific and Statistical Computing*, Vol. 12, No. 3, 1991, pp. 505-520.
7. Abraham Szöke and E. D. Brooks III,The Transport Equation in Optically Thick Media, to appear in the *JQSRT*
8. D. Mihalas, *Stellar Atmospheres*, W. H. Freeman and Company, San Francisco, 1978.
9. M. S. McKinley, E. D. Brooks III and A. Szöke, Comparison of Implicit and Symbolic Implicit Monte Carlo Line Transport with Frequency Weight Extension, *Journal of Computational Physics*, Vol. 189 (2003), pp. 330-349.

This work was performed under the auspices of the U. S. Department of Energy by University of California, Lawrence Livermore National Laboratory under contract No. W-7405-Eng-48.